Signature: © Pol J Radiol, 2017; 82: 607-611
DOI: 10.12659/PJR.903021

Polish Journal of Radiology
www.PolRadiol.com
CASE REPORT

Received: 2016.12.24
Accepted: 2017.01.22
Published: 2017.10.20

Detailed Imaging Findings in a Rare Case of Kimura Disease, with Special Mention on Diffusion Weighted Imaging

Authors' Contribution:
A Study Design
B Data Collection
C Statistical Analysis
D Data Interpretation
E Manuscript Preparation
F Literature Search
G Funds Collection

Moinullah Syed[ABCDEFG], **Divya Bhattacharya**[ABDG], **Bikash Parida**[CDF], **Ashok Sharma**[BG]

Department of Radiodiagnosis, Byramjee Jeejeebhoy Government Medical College and Sassoon General Hospitals, Poona, Maharashtra, India

Author's address: Moinullah Syed, Department of Radiodiagnosis, Byramjee Jeejeebhoy Government Medical College and Sassoon General Hospitals, Poona, Maharashtra, India, e-mail: moin.bmc@gmail.com

Summary

Background: Kimura disease is an uncommon, benign, chronic, idiopathic disease that is seen mainly in the Asian population, particularly in females. It mainly affects the salivary glands and in particular parotid and cervical lymph nodes. So far, the diagnosis of Kimura disease has been based on histopathology. We hereby report of a confirmed case of Kimura disease and provide a detailed explanation of its imaging features with a special emphasis on diffusion-weighted imaging, as diffusion sequences may help distinguish Kimura disease from malignancy.

Case Report: A middle-aged female patient presenting with a history of multiple chronic neck swellings was thoroughly evaluated by ultrasound (US), computed tomography (CT), and magnetic resonance imaging (MRI). The imaging findings included gross enlargement of the left parotid gland, a focal lesion in the right parotid gland, and cervical lymphadenopathy. These features correlated with histopathological findings, and the diagnosis of Kimura disease was made.

Conclusions: The imaging findings were found to be specific for Kimura disease.

MeSH Keywords: Angiolymphoid Hyperplasia with Eosinophilia • Diffusion Magnetic Resonance Imaging • Magnetic Resonance Imaging

PDF file: http://www.polradiol.com/abstract/index/idArt/903021

Background

Kimura disease is a rare, chronic, inflammatory disorder of an unknown etiology. It manifests as multiple subcutaneous masses in the head and neck region due to cervical lymphadenopathy and salivary gland enlargement. Most cases of Kimura disease have been reported in the Asian population, particularly in south-east Asia. However, most studies on Kimura disease deal mainly with histopathological aspects, and there is scarce literature on the imaging features of the disease due to their low specificity. The objective of this case report was to explain in detail the imaging findings in Kimura disease with a description of diffusion characteristics of the lesions. Histopathological findings that support the diagnosis are also briefly discussed.

Case Report

A 35-year-old female patient of Marathi Indian ethnicity was referred to our department with complaints of multiple swellings in both sides of the neck and in the left preauricular region for two years. On an ultrasound examination [(US), Philips HD11XE], the left parotid gland was massively enlarged and showed heterogeneous echotexture (Figure 1). On color Doppler, few prominent vessels with a low-resistance arterial waveform were seen (Figure 2). The right parotid gland also contained a focal lesion with similar echogenicity. Also, multiple enlarged cervical lymph nodes were seen at level I, II, III, and IV on the left side, and at level II and III on the right, with preserved central hilum and increased hilar vascularity on color Doppler (Figure 3). On plain CT (Siemens SOMATOM Definition AS 64x2 slice), the left parotid gland appeared enlarged and

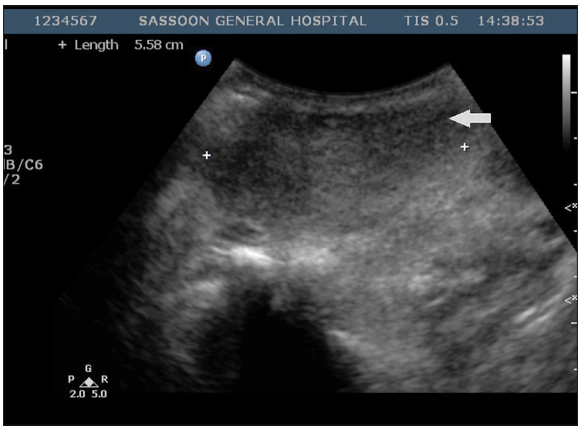

Figure 1. Low-frequency US image shows an enlarged left parotid gland with heterogeneous echotexture (arrow).

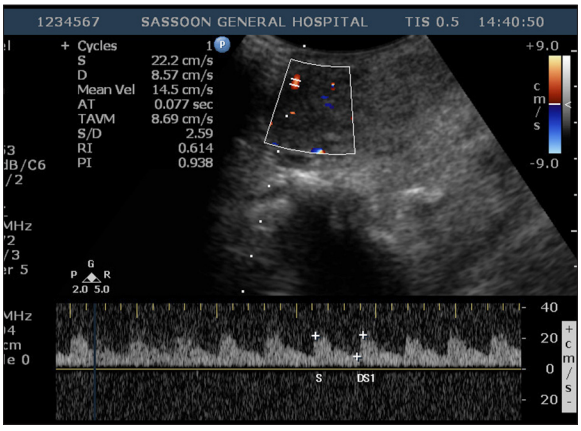

Figure 2. Color Doppler image of an enlarged gland shows few prominent vessels with low-resistance arterial waveforms.

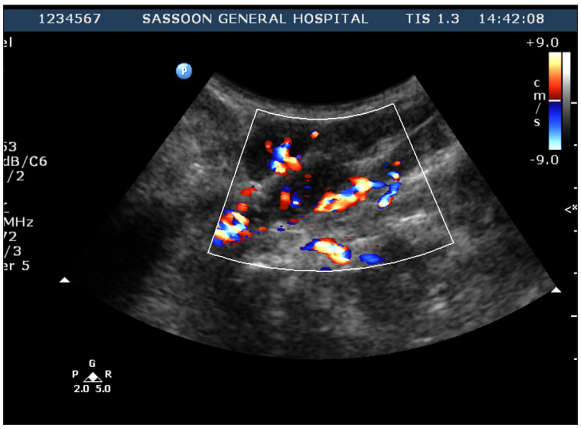

Figure 3. High-frequency US image shows enlarged cervical lymph nodes with preserved central fatty hilum and increased hilar vascularity.

homogenously hypodense (Figure 4). A focal lesion with similar density was also noted in the right parotid gland. A contrast-enhanced scan showed heterogeneous enhancement of the left parotid gland. The enlarged lymph nodes showed homogenous intense enhancement without necrosis (Figure 5). No encasement/invasion of adjacent structures around the parotid was seen. On MRI (GE Signa HDxt 1.5 Tesla), the left parotid gland and lymph nodes

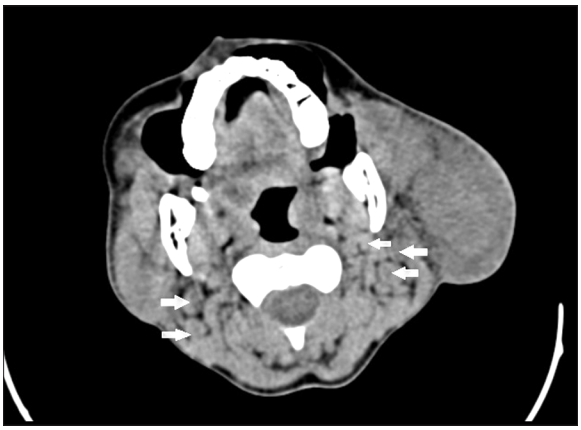

Figure 4. Plain axial CT image at the level of oropharynx shows an enlarged, isodense left parotid gland and enlarged cervical lymph nodes (arrows).

Figure 5. Coronal reformatted contrast CT image of the neck reveals heterogeneous enhancement of the left parotid gland (thick arrow) and homogenous enhancement of involved lymph nodes (thin arrows).

appeared isointense on T1W images (Figure 6), hyperintense on T2W and STIR images (Figures 7, 8), and showed enhancement on post-contrast T1W images (Figure 9). The left parotid gland appeared more heterogeneous on T2W and STIR images, with patchy enhancement on post-contrast sequences. In contrast, the lymph nodes showed a more homogenous pattern. The enlarged lymph nodes showed bright signal on diffusion-weighted imaging (DWI), with reduced apparent diffusion coefficient (ADC) values (0.00071×10^{-3} mm^2/s) at b value of 800. In contrast, the left parotid gland and the focal lesion in the right parotid gland

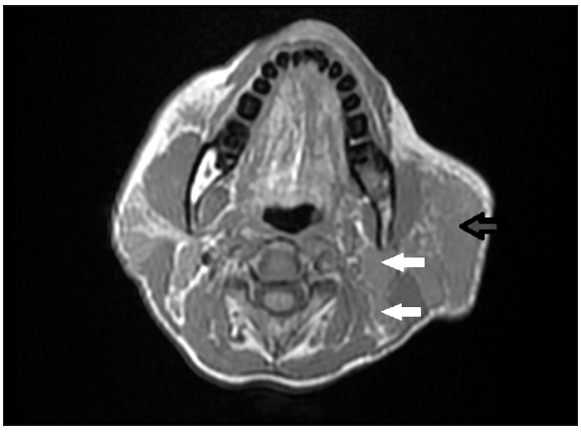

Figure 6. Axial T1W MRI image at same level as in Figure 4 shows an isointense left parotid gland (black arrow) and involved lymph nodes (white arrows).

Figure 7. Axial T2W image at the same level shows a heterogeneously hyperintense left parotid gland (black arrow) and homogenously hyperintense lymph nodes (white arrows).

showed dark signal on DWI, with increased ADC values (0.00199×10^{-3} mm^2/s) (Figures 10, 11).

The patient had an increased level of leucocytes (14,000/mm^3) and eosinophilia (45%). The patient underwent left parotidectomy with dissection of lymph nodes for suspected lymphoma. The specimens were stained with hematoxylin and eosin (H&E) and examined microscopically. The parotid specimen showed multiple areas of fibrosis with dense mononuclear infiltrate and multiple proliferative lymphoid follicles. All dissected lymph nodes showed reactive lymphoid hyperplasia and well-formed mantle zones without loss of nodal architecture. Dense mononuclear, particularly eosinophilic, cell infiltrate was noted (Figures 12, 13).

Discussion

Kimura disease, first reported as early as in 1937, was described in detail by Kimura in 1948 [1]. However, to date, only around 150 cases have been reported. It is a rare, chronic, infiltrative disease of an unknown etiology, possibly an allergic reaction to *Candida albicans* [2]. It is characterized by painless cervical lymphadenopathy and enlargement of salivary glands. Axillary and inguinal nodes

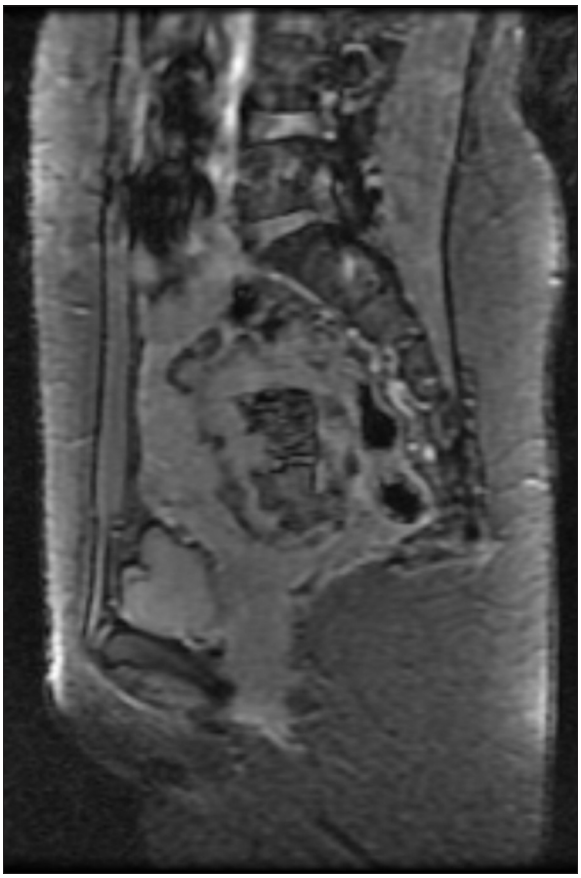

Figure 8. Coronal STIR image shows hyperintense signal of involved areas.

Figure 9. Axial post-contrast T1W image reveals heterogeneous enhancement of the left parotid gland (black arrow) and homogenous enhancement of involved nodes (white arrows).

are also reported to be affected in some cases. Nephrotic syndrome and disseminated intravascular coagulation have also been reported, underscoring the need for accurate diagnosis of Kimura disease [3,4].

Imaging features on US are non-specific. The salivary glands, particularly the parotid, appear enlarged and show heterogeneous echotexture, more often hypoechoic, mimicking neoplasm, particularly lymphoma. Few prominent

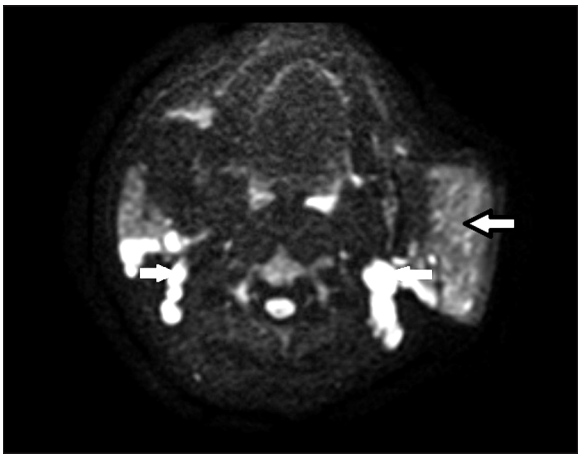

Figure 10. Axial DW image at b value of 800 shows decreased signal of the left parotid gland and increased signal in involved nodes.

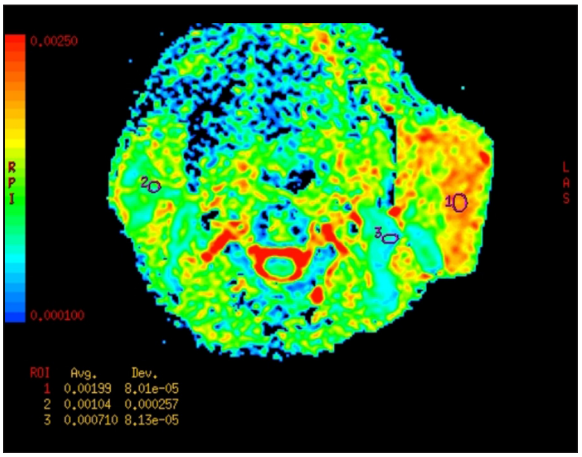

Figure 11. Color-coded ADC map at the same level shows increased diffusivity of the left parotid gland and restricted diffusion of involved nodes.

vessels with arterial waveforms can be seen within the salivary glands. The involved lymph nodes appear enlarged, with preserved central fatty hila, and show increased hilar vascularity. US is also helpful in guiding the biopsy of these lymph nodes. On CT, the enlarged salivary glands appear homogenously hypodense and show heterogeneous enhancement on post-contrast images [5]. In contrast, the enlarged lymph nodes show homogenous intense enhancement on contrast study without necrosis.

With the advantage of better soft tissue resolution and diffusion imaging, MRI is the imaging modality of choice in Kimura disease [6]. The salivary gland lesions appear iso- to hypointense to skeletal muscles on T1W images, heterogeneously hyperintense on T2W and STIR images, and enhance heterogeneously on post-contrast images. This is due to variable degrees of fibrosis within a single lesion. On the other hand, the involved lymph nodes appear more homogenous due to reactive hyperplasia. Diffusion features of the lesions are very poorly documented [7]. Only one study by Wang et al. has investigated diffusion imaging of Kimura disease, in which the ADC values of parotid lesions were higher in comparison to those of normal parotid

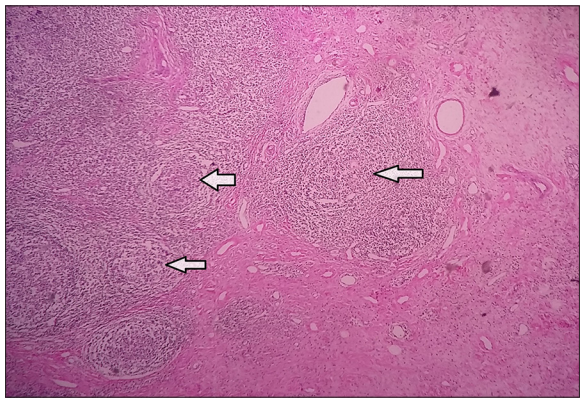

Figure 12. Low-power (10× magnification) histopathologic section of the excised specimen after H&E staining shows multiple lymphoid follicles (arrows) with intervening areas of fibrosis.

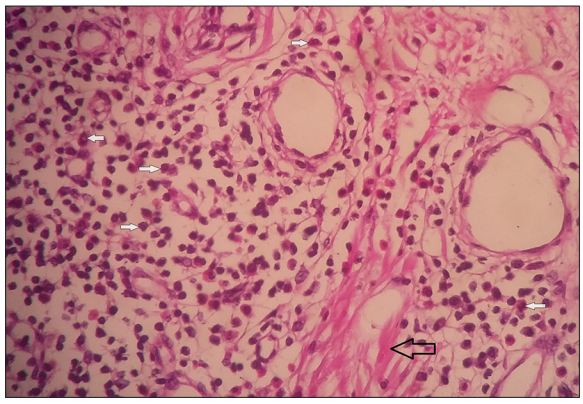

Figure 13. High-power (40× magnification) histopathologic section of the same slide shows numerous eosinophils (closed arrows) and multiple areas of fibrosis (open arrow) in addition to lymphoid infiltrate.

glands, and the ADC values of enlarged lymph nodes were much lower [8]. Similarly, in our case, the parotid lesions showed increased diffusivity with higher ADC values compared to the contralateral normal gland. In contrast, the enlarged lymph nodes showed restricted diffusion with lower ADC values compared to uninvolved nodes. This unique paradoxical diffusion feature pointed towards the diagnosis of Kimura disease rather than neoplasia, in which the parotid gland usually shows lower ADC values.

Laboratory findings that are observed in Kimura disease include peripheral eosinophilia and increased blood immunoglobulin E levels. A definite diagnosis of Kimura disease is by histopathology, where dense lymphoid proliferation with extensive mononuclear, particularly eosinophilic, infiltration and variable fibrosis are noted.

Treatment of Kimura disease is primarily surgical. However, in case of recurrence, systemic corticosteroids or local radiotherapy may be necessary.

Differential diagnosis of Kimura disease includes lymphoma, metastases, tuberculosis, other granulomatous disorders, parotid neoplasms, and angiolymphoid hyperplasia with eosinophilia (ALHE). Proper clinical history

with imaging and pathological findings is needed for specific diagnosis. In case of lymphoma, on MRI, the involved glands show signal similar to that found in Kimura disease on T1 and T2W images; however, they also show restricted diffusion with decreased ADC values. Other infiltrative parotid neoplasms show varying signal intensity on T1W and T2W images, may or may not show restricted diffusion, and usually show homogenous enhancement. Imaging features of tuberculosis and other granulomatous diseases on MRI are low T1 and high T2 signal of the involved glands with heterogeneous contrast enhancement. Presence of necrotic and calcified lymph nodes further points towards the diagnosis of tuberculosis. Although previously thought to be a subtype of ALHE, Kimura disease is now considered a separate entity, as ALHE affects skin but not lymph nodes.

Conclusions

Although primary diagnosis of Kimura disease is pathological, diffusion-weighted imaging with ADC value correlation is an important tool alongside conventional MRI and CT for a proper diagnosis. The contrast in the ADC values between the parotid glands and lymph nodes is a specific finding and should be a take-home message with respect to diagnosing Kimura disease.

References:

1. Kimura T, Yoshimura S, Ishikawa E: On the unusual granulation combined with hyperplastic changes of lymphatic tissues. Trans Soc Pathol Jpn, 1948; 37: 179–80
2. Ohta N, Fukase S, Suzuki Y et al: Increase of Th2 and Tc1 cells in patients with Kimura's disease. Auris Nasus Larynx, 2011; 38(1): 77–82
3. Othman SK, Daud KM, Othman NH: Kimura's disease: A rare cause of nephrotic syndrome with lymphadenopathy. Malays J Med Sci, 2011; 18(4): 88–90
4. Saini A, Singh V, Chandra J, Dutta AK: Kimura's disease: An unusual glandular involvement with blood and tissue eosinophilia. Indian J Pediatr, 2009; 76: 647–48
5. Anil G, Tan TY: Kimura's disease: Imaging patterns on computed tomography. Clin Radiol, 2009; 64: 994–99
6. Park SW, Kim HJ, Sung KJ et al: Kimura disease: CT and MR imaging findings. Am J Neuroradiol, 2012; 33(4): 784–88
7. Horikoshi T, Motoori K, Ueda T et al: Head and neck MRI of Kimura disease. Br J Radiol, 2011; 84(1005): 800–4
8. Wang J, Tang Z, Feng X et al: Preliminary study of diffusion-weighted imaging and magnetic resonance spectroscopy imaging in Kimura disease. J Craniofac Surg, 2014; 25(6): 2147–51